Journal of Ceramic Processing Research. Vol. 16, No. 5, pp. 462~467 (2015)

J O U R N A L O F
Ceramic Processing Research

Optimized synthesis of carbon nanotubes using a zeolite template

Wei Zhao[a], Dong Nam Seo[b], Sukyoung Kim[a,*] and Ik Jin Kim[b,*]

[a]*School of Materials Science & Engineering, Yeungnam University, Gyeongsan city, Gyeongbuk, 712-749,Korea*

[b]*Department of Materials Science and Engineering, Hanseo University, 360 Daegok-ri, Haemi-myun, Seosan city, Chungnam, 356-706, Korea*

Fe-, Co-, Ni-, and Cu-supported zeolite (FAU) crystals were prepared respectively to synthesize carbon nanotubes (CNTs) using catalytic chemical vapor deposition (CCVD) method. To avoid the massive oxidation of metal elements which can be harmful to the stabilization of the zeolite crystals, Fe-, Co-, Ni-, and Cu-supported zeolite was calcined under N_2 to obtain the re quired catalysts. CNT synthesis was performed under different conditions by varying the synthesis parameters, such as the catalysts, reaction temperature, reaction duration period, and carbon precursor feeding rate. The optimal reaction conditions for CNT synthesis was examined by comparing the quality of the CNTs synthesized under a range of conditions.

Key words: Carbon nanotubes, Chemical vapor deposition, Zeolite, Ion-exchange, Catalyst.

Introduction

Due to their unique nanostructure-dependent physical and chemical properties [1-2], Carbon nanotubes (CNTs) have found potential applications in various areas, such as nanoelectronic devices [3], composite materials [4], and hydrogen storage media [5]. Since the first report by Iijima [6], progress on CNTs has evolved at a very rapid rate, starting with the methods for producing them.

For now, a multitude of techniques with different basic principles have been developed, mainly including arc discharge method [7], laser ablation [8], and chemical vapor deposition (CVD) [9]. CVD has proven to be more effective than other methods due to its low cost, easy manipulation, and possibility of massive production with high purity. In particular, catalytic CVD (CCVD) is a medium temperature (700-1473 K) and long-time reaction (typically minutes to hours) technique, which uses transition metal particulate catalysts (Fe, Co, Ni or their binary mixtures or related oxides). One more important advantage of this technique over the other two is that the CNT synthesis from CCVD can be realized on a conventional or patterned substrate [10-11].

In principle, with their size decreasing to nanoscale, transition metal particles have a strong agglomeration tendency. Therefore, maintaining the morphology and size of these particles at the CVD processing temperatures is essential to the characteristics of synthesized CNTs, such as thickness, uniformity, and yield [12]. Therefore, catalytic supports or matrices, such as alumina [13], mesoporous silica [14], and zeolites [15], have been used to prevent the agglomeration of catalyst nanoparticles (NPs). Among them, zeolites are considered excellent hosts for supporting or encapsulating the catalyst NPs because of their well-defined pore structures and high surface areas [16], thereby leading to catalyst particle stabilization, producing a fine dispersion of catalyst particles, and increasing the number of nucleation sites, which is advantageous to the high yield synthesis of CNTs [17]. On the other hand, few studies have examined methods of controlling the synthesis parameters to determine the optimal conditions for CNT synthesis using zeolite as a template.

In this study, faujasite-type zeolite NaX (FAU) was used as a support for the metal catalyst NPs using a simple ion-exchange method in an aqueous solution to produce the catalysts for the CVD synthesis of CNTs. In contrast to another study [18], the calcination of metal-support zeolite under N_2 protection at 723 K was performed to avoid massive oxidation of the exchanged metal NPs, aiming to stabilize the zeolite structure from collapse. To the best of the authors' knowledge, this process was proposed and described briefly in a previous study [19]. The dependence of the CNT products on the synthesis parameters was examined in detail by varying the catalysts, reaction temperature, reaction duration, and carbon precursor feeding rate. The optimal synthetic conditions were then determined by comparing between the CNT products synthesized under a range of conditions.

Experimental

Materials

Iron(II)-chloride tetrahydrate ($FeCl_2 \cdot 4H_2O$, ≥ 99.0%), and

*Corresponding author:
Tel : +82-660-1441
Fax: +82-660-1402
E-mail: ijkim@hanseo.ac.kr, sykim@yu.ac.kr

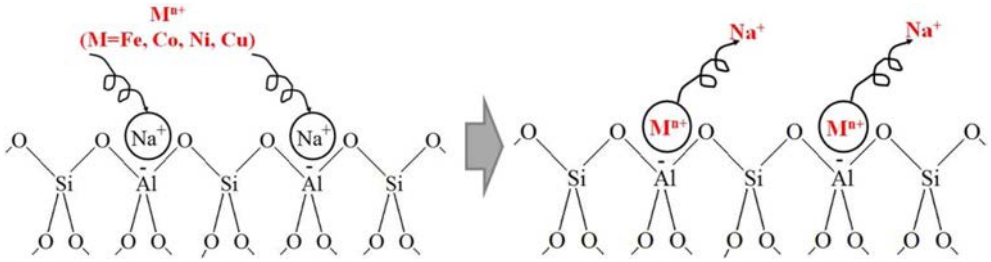

Fig. 1. Schematic diagram of the ion-exchange mechanism between the metal ions (Fe^{2+}, Co^{2+}, Ni^{2+}, and Cu^{2+}) and zeolite NaX.

cobalt(II)-chloride hexahydrate ($CoCl_2 \cdot 6H_2O$, ≥ 97.0%) were purchased from SANCHUN. Nickel chloride tetrahydrate ($NiCl_2 \cdot 4H_2O$, ≥ 98.5%), and copper (II) chloride dihydrate ($CuCl_2 \cdot 2H_2O$, ≥ 99.0%) were purchased from Sigma-Aldrich. All materials were used as received.

Preparation of the Fe- and Co-supported zeolite catalysts

Zeolite NaX (FAU) crystals, 15 μm in size, were synthesized hydrothermally using a method described preciously [20]. First, a certain amount of $FeCl_2 \cdot 4H_2O$, $CoCl_2 \cdot 6H_2O$, $NiCl_2 \cdot 4H_2O$, and $CuCl_2 \cdot 2H_2O$ (0.08 mol%, 0.12 mol%, 0.16 mol%, and 0.20 mol%) was respectively dissolved in 250 mL of deionized water by magnetic stirring. Then, the zeolite powder of 1 g was respectively mixed with these solutions with vigorous stirring for 24 hours under ambient condition. Subsequently, the mixture was centrifuged, and washed thoroughly with anhydrous ethanol. Using ethanol instead of water is to prevent the exchanged metal ions from dissolving into the water and being lost during the washing process. Finally, the powder was vacuum dried at ambient temperature and calcined at 723 K under nitrogen (N_2) flow for 3 hours prior to the CNT synthesis. Fig. 1 shows a schematic diagram of the mechanism for the ion-exchange process. The Fe-, Co-, Ni-, and Cu-supported zeolite samples were designated $FeX(N_2)$, $CoX(N_2)$, $NiX(N_2)$, and $CuX(N_2)$, respectively.

Synthesis of CNTs

The CNTs were synthesized by the catalytic decomposition of C_2H_2 on the calcined Fe- and Co-supported zeolite in a fixed-bed flow reactor under atmospheric pressure. The reactor setup consisted of a quartz boat containing the catalyst sample (~ 100 mg), which was placed in a horizontal electric tubular furnace. The catalysts were heated gradually from room temperature to 973 K in flowing nitrogen (N_2, 500 sccm) and kept at this temperature for approximately 15 min. During the subsequent reaction, a mixture of N_2 (200 sccm) and C_2H_2 (5, 10, and 15 sccm) was fed into the reactor for 5, 10, 15, and 30 minutes. The furnace was then cooled to room temperature under flowing N_2 (500 sccm) and the CNTs produced were collected as a black powder from a quartz boat.

Characterization

Field emission SEM (FESEM, FESEM LEO 1530 VP) was performed at an acceleration voltage of 1.0 kV. High resolution transmission electron microscopy (HRTEM, JEOL JEM-3011) was conducted at an acceleration voltage of 200 kV. Powder X-ray diffraction (XRD, Rigaku D/max 2500 VL/PC) was performed using Cu Ká radiation (40 kV, 40 mA, k = 1.5418 Å). The patterns were recorded from 10 to 70 ° 2θ in 0.04 ° steps with a counting time of 2 s per step. Thermogravimetric analysis (TGA, Seiko Extar 7300, TG/DTA 7300) was performed to measure the amount of carbon deposited in the experiment with ≈5 mg samples heated in air from 298 K to 1073 K at a heating rate of 10 K/min. Raman spectroscopy (Raman system FRA-106/S) was performed using a laser excitation line at 1064 nm (Nd-YAG).

Result and Discussion

Effect of the metal catalysts

According to a previous report [21], carbon products with distinct morphologies can be obtained using different metal (Fe, Co, Ni, and Cu)-supported zeolites as the catalyst.

A homogeneous distribution of metal nanoparticles was observed for both Ni and Cu, even with different levels of clustering, as observed by HRTEM (data not shown). A mixture of quasi-carbon nanofibers (CNFs) with a belt-like wall structure and CNTs were both obtained from Ni, with the former being the main products, whereas graphene sheets were produced mainly from Cu, which can be confirmed by their transparent features and dark vein-like structures.

On the other hand, from Fe and Co, only multi-walled CNTs (MWCNTs) were the main products. Therefore, the following sections will focus on the CNTs synthesized from Fe- and Co-supported zeolite catalysts. The CNTs synthesized from Co showed higher quality (fewer defects, clearer wall layer structure and much more homogeneously-distributed diameter) than those obtained from Fe, as confirmed by TEM (data not shown) and Raman spectroscopy (data not shown) [21].

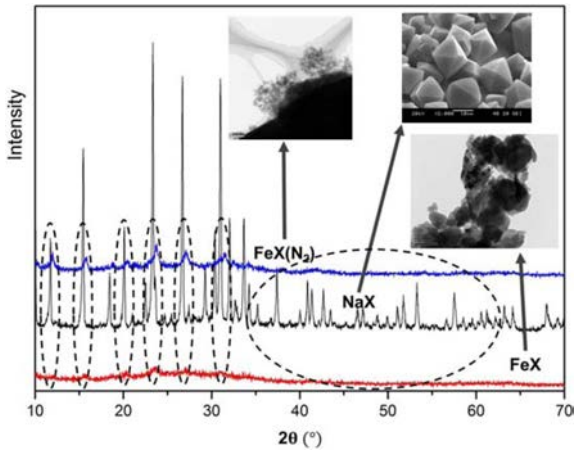

Fig. 2. XRD pattern of the NaX, FeX, and FeX(N_2) samples (insets showing the corresponding TEM and SEM images).

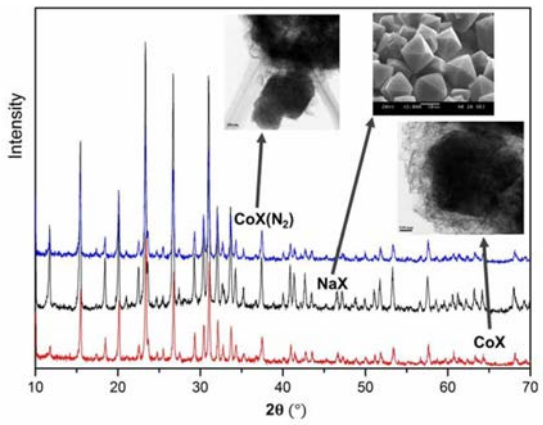

Fig. 3. XRD pattern of the NaX, CoX, and CoX(N_2) samples (insets showing the corresponding TEM and SEM images).

Characterization of calcined Fe- and Co-supported Zeolite catayst

Figs. 2 and 3 show XRD patterns of pristine zeolite crystals, and Fe- and Co-exchanged zeolite catalysts calcined in air and N_2, respectively.

Compared to the pristine zeolite crystals, the Fe-supported zeolite samples calcined in air or N_2 showed peaks with a considerably reduced intensity at the characteristic 2θ positions for original zeolite (Fig. 2). This suggests that the zeolite crystal structure had collapsed after calcination regardless of the atmosphere. This is highlighted by the irregular shape edge, as shown in the insets in Fig. 2. Moreover, the characteristic peaks marked by dash-line ovals in Fig. 2 showed a slight shift toward higher 2θ values, indicating a change in the zeolite crystal structure. In addition, the FeX(N_2) sample still showed sharp characteristic peaks corresponding to zeolite NaX but there was no single peak for the FeX sample calcined in air, which highlights the role of N_2 in stabilizing the zeolite structure. In the case of the Co-supported zeolite samples, the characteristic peaks at the same 2θ positions as those of pristine zeolite crystals in the XRD patterns were still as sharp and intense after calcination regardless of the atmosphere, which could be explained by the excellent stabilization of the zeolite structure. This can be confirmed by the distinct shape edge, as shown in the insets in Fig. 3. Furthermore, no shifts in the XRD patterns were observed, which can also be proof of the maintenance of the zeolite crystal structure.

These results suggest that Co is a better metal choice than Fe for producing metal-supported zeolite catalysts without collapsing the zeolite structure. In addition, calcination in N_2 was more effective in stabilizing the metals in the zeolite than calcining in air.

Impact of the reaction temperature

Figs. 4 and 5 show TEM images of the carbon products synthesized from the FeX(N_2) and CoX(N_2) catalysts , respectively, at 973 K, 1073 K, 1173 K, and 1273 K.

In the case of the carbon products catalyzed by the FeX(N_2) catalyst, the CNTs were formed at relatively low temperatures (Fig. 4(a)), showing a clear wall structure, but the outermost layer still showed amorphous carbon, as shown in the inset. With increasing temperature, the wall structure became more defective, but still maintained a tubular shape (Fig. 4(b) and its inset), and the defects increased gradually as the temperature was increased, as confirmed by the appearance of amorphous carbon-capped catalyst clusters and belt-like products, as shown in Fig. 4(c) and its inset. When the temperature reached 1273 K, there were no signs of tubular-like products and large clusters encapsulated with a thick layer of amorphous carbon, as shown in Fig. 4(d).

A similar variation tendency was observed for the carbon products catalyzed by the CoX(N_2) catalyst, as shown in Fig. 5(a)-(d) and their corresponding insets. In addition, at lower temperatures (973 K) where only CNTs were obtained, the CNTs synthesized from CoX(N_2) were thinner with fewer defects than those from FeX(N_2).

The results analyzed above can be explained as follows. The melting point of zeolite NaX is probably more than 973 K due to the collapsed zeolite structure, as shown by the TEM images in Figs. 4 and 5. With increasing temperature, the catalyst NPs that were originally well-stabilized in zeolite began to come in contact with each other because of the gradual collapse of the zeolite structure. During the CVD process at elevated temperatures, the metal NPs agglomerated to form larger clusters. They lost their catalytic activity when a certain size was reached [22], and the CNTs were no longer favorable products because large clusters are not beneficial to the synthesis of CNTs but formed amorphous carbon instead [23]. Therefore, at 1273 K, the zeolite structure was completely destroyed, leading to the formation of amorphous carbon only. Moreover, the amorphous carbon capped clusters

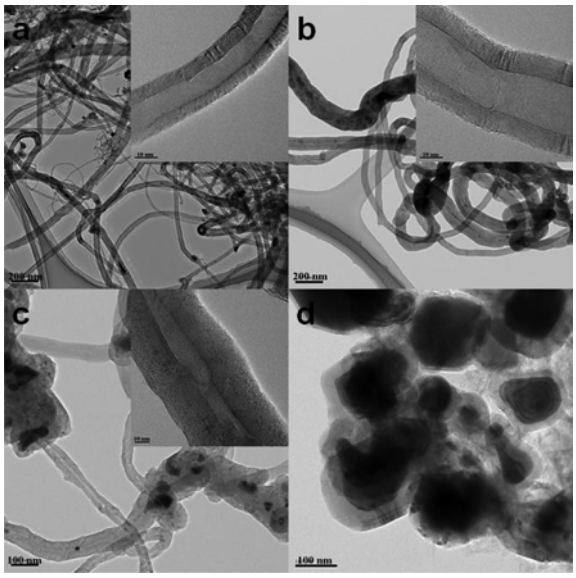

Fig. 4. TEM images of the CNTs synthesized from $FeX(N_2)$ at different temperatures: (a) 973 K, (b) 1073 K, (c) 1173 K, and (d) 1273 K.

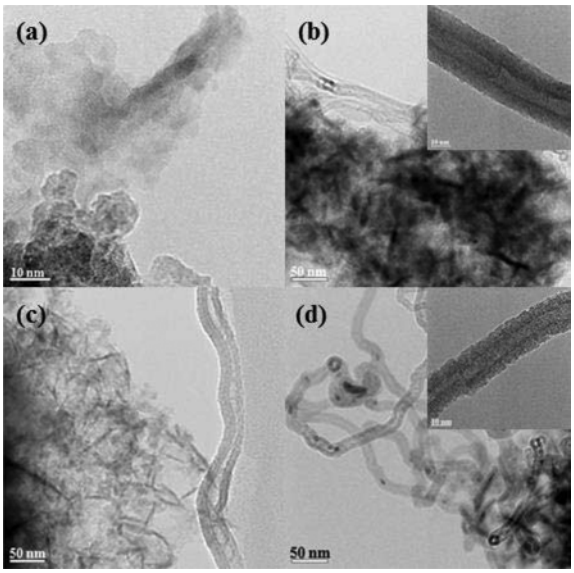

Fig. 6. TEM images of the CNTs synthesized from the $FeX(N_2)$ at different reaction times: (a) 5 min, (b) 10 min, (c) 15 min, and (d) 30 min.

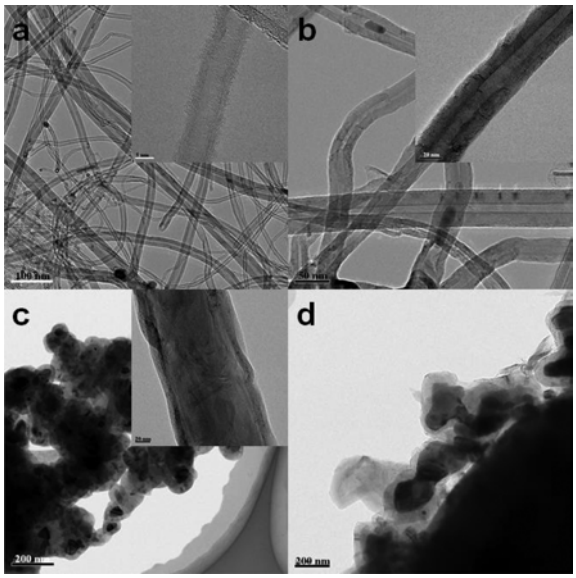

Fig. 5. TEM images of the CNTs synthesized from $CoX(N_2)$ at different temperatures: (a) 973 K, (b) 1073 K, (c) 1173 K, and (d) 1273 K.

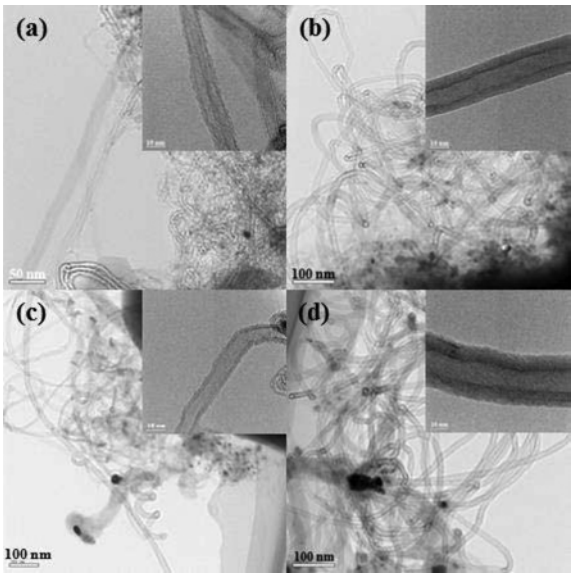

Fig. 7. TEM images of the CNTs synthesized from the $CoX(N_2)$ at different reaction times: (a) 5 min, (b) 10 min, (c) 15 min, and (d) 30 min.

synthesized by $CoX(N_2)$ were much larger than those synthesized by $FeX(N_2)$, as shown in Figs. 4(d) and 5(d), suggesting that Fe has a stronger agglomerating tendency than Co.

Effect of the reaction time

The effect of the reaction time on the CNT products was examined with the reaction temperature fixed to 973 K, the optimal temperature. Figs. 6 and 7 show TEM images of the CNT products synthesized from the $FeX(N_2)$ and $CoX(N_2)$ catalysts, respectively.

Within a short reaction period, such as 5 minutes, no CNTs were formed from the $FeX(N_2)$ catalyst (Fig. 6(a)). With increasing reaction time, CNTs with many defects together with unreacted carbon-capped amorphous products were produced from the $FeX(N_2)$ catalyst, as shown in Fig. 6(b) and (c). When the reaction time was increased to 30 minutes, the products were mainly MWCNTs but defects were unavoidable, as shown in Fig. 6(d).

A completely different result was obtained in the case of the CNTs synthesized by the $CoX(N_2)$ catalyst, where ultra-thin CNTs were obtained even in a very short reaction period, 5 minutes, as shown in Fig. 7(a) and the inset. This suggests that $CoX(N_2)$ might have higher catalytic ability than $FeX(N_2)$ and can catalyze CNT

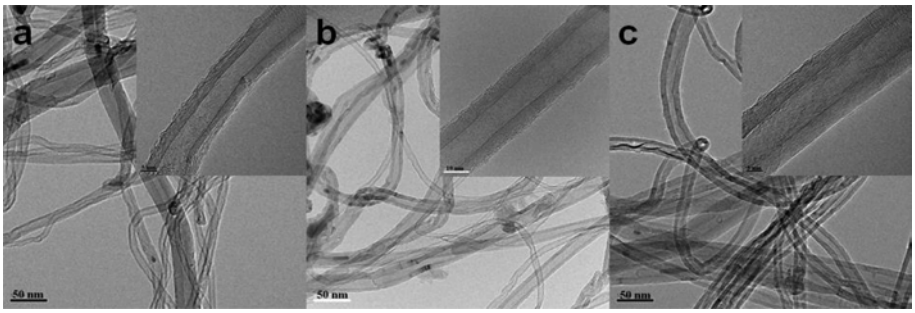

Fig. 8. TEM images of the CNTs synthesized from the $FeX(N_2)$ catalyst at different C_2H_2 flow rates at 973 K: (a) 5 sccm, (b) 10 sccm, and (c) 15 sccm.

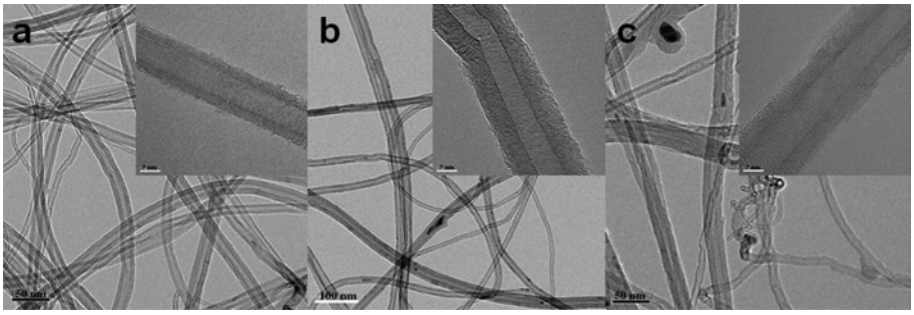

Fig. 9. TEM images of CNTs synthesized from the $CoX(N_2)$ catalyst at different C_2H_2 flow rate at 973 K: (a) 5 sccm, (b) 10 sccm, (c) 15 sccm.

synthesis more easily within a very short period. When the reaction time was increased to 10 and 15 minutes, the yield of the CNTs was increased significantly, and their diameter showed an increasing tendency, as shown in Fig. 7(b) and (c) and their corresponding insets, respectively. After a 30 minute reaction, relatively thick MWCNTs with more defects were observed, as shown in Fig. 7(d) and its inset.

Therefore, $CoX(N_2)$ was found to be more beneficial for CNT synthesis than $FeX(N_2)$, particularly in the synthesis of ultra-thin CNTs, such as single-walled CNTs, double-walled CNTs and triple-walled CNTs. Moreover, thin CNTs were very difficult to synthesize using the latter catalyst.

Effect of carbon precursor flow rate

In addition to the reaction temperature and reaction time, the effect of the carbon precursor flow rate was examined. Figs. 8 and 9 show TEM images of the CNTs synthesized from $FeX(N_2)$ and $CoX(N_2)$, respectively, under different C_2H_2 flow rates.

TEM images of the CNTs synthesized from $FeX(N_2)$, shown in Fig. 8(a)-(c) and their corresponding insets showed that a higher C_2H_2 flow rate led to CNTs with larger diameters (including the inner and outer diameters). Interestingly, the CNTs synthesized at a C_2H_2 flow rates of 5 and 15 sccm showed much lower quality than those synthesized at 10 sccm, including more defects and a wider distribution of diameters.

In contrast, the CNTs synthesized from $CoX(N_2)$, as shown in Fig. 9(a)-(c) and their corresponding insets, showed fewer defects and a more complete wall

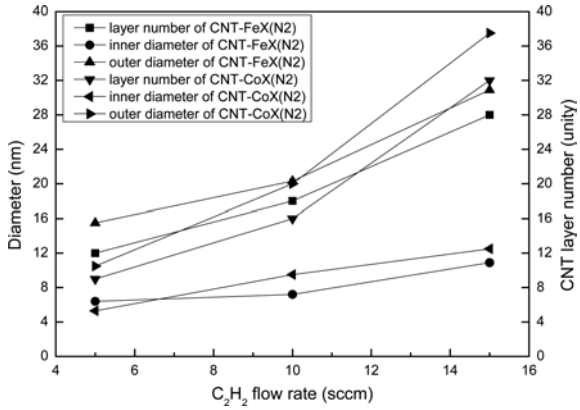

Fig. 10. Correlation between the C_2H_2 flow rate, and the mean inner and outer diameters, as well as the number of carbon layers of the CNTs synthesized from the $FeX(N_2)$ and $CoX(N_2)$ catalysts.

structure, indicating higher crystallinity compared to those synthesized from $FeX(N_2)$. The change in diameter showed a similar increasing tendency with increasing C_2H_2 flow rate. Furthermore, the CNTs synthesized at relatively lower C_2H_2 flow rates, such as 5 and 10 sccm, possessed a distinct multi-wall structure, whereas at a higher C_2H_2 flow rate, e.g. 15 sccm, the wall structure appeared ambiguous, which was different from those synthesized from $FeX(N_2)$. This shows that Co has higher catalytic ability in catalyzing CNT synthesis than Fe, thereby requiring only a small amount of C_2H_2 per unit time. Therefore, a much larger C_2H_2 rate can result in an over-reaction as well as the formation of more decomposed carbon as

defects covering the surface.

Fig. 10 presents the correlation between the mean inner and outer diameters, and the number of carbon layers of the CNTs synthesized from $FeX(N_2)$ and $CoX(N_2)$ catalysts, and the C_2H_2 flow rate.

For both catalysts, the CNT products showed an increasing tendency in their inner and outer diameters, and the wall layer number increased with increasing C_2H_2 flow rate, corresponding to the results obtained from Figs. 8 and 9. At a much higher rate, e.g. 15 sccm, the inner and outer diameters, and the number of wall layers of the CNTs synthesized from $CoX(N_2)$ were both larger than those synthesized from $FeX(N_2)$. On the other hand, at a lower rate, e.g. 5 sccm, the CNTs synthesized from $CoX(N_2)$ had smaller inner and outer diameters, as well as a smaller number of wall layers than those synthesized from $FeX(N_2)$. In contrast, at an intermediate rate (10 sccm), the CNTs synthesized from both $CoX(N_2)$ and $FeX(N_2)$ were similar. This suggests that at a relatively low carbon precursor feeding rate, the synthesized CNTs showed smaller diameters (including inner and outer diameters) from the $CoX(N_2)$ catalyst because $CoX(N_2)$ had higher catalytic ability and better dispersion as well as relatively unchanged metal NP size compared to $FeX(N_2)$. When the feeding rate exceeded a certain point, the reaction rate of CNTs on the $CoX(N_2)$ catalyst was too high [24], resulting in a much larger CNT diameter and wall layer number. Therefore, 10 sccm appears to be most suitable for the synthesis of highly crystalline CNTs.

Conclusions

Different metal ions exchanged with zeolite NaX can lead to different carbon products under the same CVD reaction conditions, such as CNTs from Fe and Co, mixture of CNTs and CNFs with belt-like outer layer structure from Ni, and graphene sheets from Cu.

N_2 can protect the FeX and CoX catalysts from oxidation and prevent the collapse of the zeolite structure during the calcination process. The former experienced severe zeolite structural breaking-down, whereas the latter could maintain its original structure.

The optimal temperature for CNT synthesis using metal-supported zeolite as a catalyst was approximately 973 K.

The optimal catalyst for obtaining ultra-thin CNTs was $CoX(N_2)$, and a short reaction duration period, such as 5 minutes, could lead to CNTs with few walls. With increasing reaction time, the diameter of the CNTs showed an increasing tendency.

Under a fixed temperature and appropriate reaction time, the carbon precursor flow rate played a vital role in CNT synthesis. With increasing C_2H_2 rate, the inner and outer diameter of the synthesized CNTs, as well as the number of carbon wall layers showed a monotonic increasing tendency. The optimal C_2H_2 feeding rate was found to be 10 sccm.

Co showed a greater catalytic ability for synthesizing CNTs than Fe.

Acknowledgments

This study was supported by grants from the 2013 Fundamental R&D Program of Hanseo University and from National Research Foundation of Korea (NRF).

References

1. H. Dai, J. H. Halner, A. G. Rinzler, D. T. Colbert, and R. E. Smalley, Nature 384 (1996) 147-150.
2. T. Rueckes, K. Kim, E. Joselevich, G. Y Tseng, C. L. Cheung, and C. M. Lieber, Science 289 (2000) 94-97.
3. A. Bachtold, P. Hadley, T. Nakanishi, and C. Dekker, Science 294 (2001) 1317-1320.
4. P. Calvert, Nature 399 (1999) 210-211.
5. A. C. Dillon, K. M. Jones, T. A. Bekkedahl, C. H. Kiang, D. S. Bethune, and M. J. Heben, Nature 386 (1997) 377-379.
6. S. Iijima, Nature 354 (1991) 56-58.
7. W. Kratschmer, L. D. Lamb, K. Fostiropoulos, and D. R. Huffman, Nature 347 (1990) 354-358.
8. H. W. Kroto, J. R. Heath, S. C. O'Brian, R. F. Curl, and R. E. Smalley, Nature 318 (1985) 162-163.
9. K. P. De Jong and J. W. Geus, Catal. Rev.-Sci. Eng. 42 (2000) 481-510.
10. L. Ding, D. Yuan, and J. Liu, J. Am. Chem. Soc. 130 (2008) 5428-5429.
11. M. J. Bronikowski, J. Phys. Chem. C 111 (2007) 17705-17712.
12. H. Dai, A. G. Rinzler, P. Nikolaev, A. Thess, D. T. Colbert, and R. E. Smalley, Chem. Phys. Lett. 260 (1996) 471-475.
13. Z. Konya, I. Vesselenyi, K. Lazar, J. Kiss, and I. Kiricsi, IEEE Trans. Nanotechnol. 3 (2004) 73-79.
14. W. Z. Li, S. S. Xie, L. X. Qian, B. H. Chang, B.S. Zou, W.Y. Zhou, R.A. Zhao, and G. Wang, Science 274 (1996) 1701-1703.
15. K. Hernadi, A. Fonseca, J.B. Nagy, D. Bernaerts, A. Fudala, and A. A. Lucas, Zeolites 17 (1996) 416-423.
16. M. Hulman, H. Kuzmany, O. Dubay, G. Kresse, L. Li, Z. K. Tang, P. Knoll, and R. Kaindl, Carbon 42 (2004) 1071-1075.
17. H. Ago, S. Imamura, T. Okazaki, T. Saitoj, M. Yumura, and M. Tsuji, J. Phys. Chem. B 109 (2005) 10035-10041.
18. A. Okamoto and H. Shinohara, Carbon 43 (2005) 431-436.
19. W. Zhao, D. N. Seo, A. Pokhrel, J. Gong and I. J. Kim, Journal of the Korean Ceramic Society 50 (2013) 1-17.
20. H. J. Lee and I. J. Kim, Journal of the European Ceramic Society 27 (2007) 561-564.
21. W. Zhao, H. T. Kim, and I. J. Kim, Journal of Ceramic Processing Research 13 (2012) 81-85.
22. M. Haruta, Catal. Today 36 (1997) 153-166.
23. M. H. Rümmeli, C. Kramberger, F. Schäffel, E. B. Palen, T. Gemming, B. Rellinghaus, O. Jost, M. Löffler, P. Ayala, T. Pichler, and R. J. Kalenczuk, Phys. Stat. Sol. (B) 244 (2007) 3911-3915.
24. C. J. Lee, J. H. Park, and J. A. Yu, Chem. Phys. Lett. 360 (2002) 250-255.